Mol Neurobiol (2016) 53:4798–4808
DOI 10.1007/s12035-015-9410-0

The Differentiation of Human Endometrial Stem Cells into Neuron-Like Cells on Electrospun PAN-Derived Carbon Nanofibers with Random and Aligned Topographies

Esmaeil Mirzaei[1,2] · **Jafar Ai**[3] · **Somayeh Ebrahimi-Barough**[3] · **Javad Verdi**[4] · **Hossein Ghanbari**[1] · **Reza Faridi-Majidi**[1]

Received: 23 July 2015 / Accepted: 23 August 2015 / Published online: 3 September 2015

Abstract Electrospun carbon nanofibers (CNFs) have great potential for applications in neural tissue regeneration due to their electrical conductivity, biocompatibility, and morphological similarity to natural extracellular matrix. In this study, we cultured human endometrial stem cells (hEnSCs) on electrospun CNFs with random and aligned topographies and demonstrated that hEnSCs could attach, proliferate, and differentiate into neural cells on both random and aligned CNFs. However, the proliferation, differentiation, and morphology of cells were affected by CNF morphology. Under the proliferative condition, hEnSCs showed lower proliferation on aligned CNFs than on random CNFs and on tissue culture plate (TCP) control. When cultured on aligned CNFs in neural induction media, hEnSCs showed significant upregulation of neuronal markers, NF-H and Tuj-1, and downregulation of neural progenitor marker (nestin) compared to that on random CNFs and on TCP. In contrast, hEnSCs showed higher expression of nestin and slight upregulation of oligodendrocyte marker (OLIG-2) on random CNFs compared to that on aligned CNFs and on TCP. SEM imaging revealed that differentiated cells extended along the CNF main axis on aligned CNFs but stretched multidirectionally on random CNFs. These findings suggest electrospun CNFs as proper substrate for stem cell differentiation into specific neural cells.

Keywords Electrospun carbon nanofibers · Surface topography · Human endometrial stem cell · Differentiation · Neuron-like cells

✉ Reza Faridi-Majidi
refaridi@sina.tums.ac.ir

[1] Department of Medical Nanotechnology, School of Advanced Technologies in Medicine, Tehran University of Medical Sciences, Tehran, Iran

[2] Department of Medical Nanotechnology, School of Advanced Medical Sciences and Technologies, Shiraz University of Medical Sciences, Shiraz, Iran

[3] Department of Tissue Engineering, School of Advanced Technologies in Medicine, Tehran University of Medical Sciences, Tehran, Iran

[4] Department of Applied Cell Sciences, School of Advanced Technologies in Medicine, Tehran University of Medical Sciences, Tehran, Iran

Introduction

Central nervous system (CNS) pathologies such as Alzheimer's, Parkinson's, stroke, heat stress, brain trauma, and spinal cord trauma are associated with neuron loss or dysfunction in CNS and affect a large percentage of the world's population. The number of people suffering from neuronal disorders is growing with the increasing of age and population of the world. Neuronal regeneration of CNS is challenging due to the complexity of native CNS tissue and function. Solutions to recover neurological function are still needed for all CNS injuries [1–3].

As a new approach, neural tissue engineering holds great promise for neural tissue regeneration. This emerging interdisciplinary field provides novel and improved biological substrates and scaffolds that can restore, maintain, or improve neural tissue functions [3]. Among a variety of constructs used for neural tissue engineering, nanostructures, because of their similarity to natural neural tissues (such as nanostructured extracellular matrices), have rapid expansion applications in neuroscience [4, 5].

Recently, among the variety of available nanomaterials, carbon-based nanostructures such as carbon nanotubes (CNTs) and carbon nanofibers (CNFs) have attracted great

interest in neural tissue regeneration applications due to their electrical conductivity, excellent mechanical properties, structural similarity to natural neural tissue components, and biocompatibility with neural tissue [2, 1, 6]. In this concept, CNTs/CNFs have been used as substrates/scaffolds for supporting neural cell adhesion, promoting cell growth, enhancing neuritis orientation, neuritis outgrowth and branching, and promoting differentiation of stem cells to specific neural cell lineage as well [7–11]. For example, Mattson et al. demonstrated that embryonic rat–brain neurons can adhere and extend neuritis on unmodified CNTs and CNTs coated with the bioactive molecule 4-hydroxynonenal [12]. It has also been reported that CNTs are able to improve neural signal transfer while supporting dendrite elongation and cell adhesion [13]. Increase in the efficacy of neural signal transmission was attributed to the specific properties of CNT materials, such as the high electrical conductivity. CNTs had also shown the ability to modulate differentiation of stem cells into neural cells [14, 15, 11]. It is well known that the interaction between stem cells and extracellular microenvironment is critical in controlling stem cell differentiation [16, 17].

The CNTs and CNFs that are commonly used in neurological applications are fabricated mostly by techniques including electric arc, laser ablation, and chemical vapor deposition (CVD) [2, 5]. These techniques produce CNTs/CNFs mostly as powder or as a layer deposited on a surface such as glass. To be used as substrate/scaffold suitable for tissue regeneration goals, such CNTs/CNFs need to be deposited on a surface [18, 19, 9, 12] or be composited or grafted with other materials mostly polymers [14, 20]. On the other hand, so-called CNTs/CNFs contain a substantial fraction of metal catalyst which may cause toxicity which further limits their biological applications [5].

As a new class of carbon nanostructure, electrospun carbon nanofibers, which have excellent electrical and mechanical properties along with similarity to natural extracellular matrix, provide possible candidates for neural tissue repair applications [21]. Electrospinning, a simple and rapidly developing technique, provides a straightforward approach to produce continuous (long) fibers with diameters ranging from submicrons to nanometers from diversity of polymers. Electrospun nanofibers have structural features similar to natural extracellular matrix and have been widely used as tissue engineering scaffold [22]. Subsequently, carbon nanofibers (CNFs) can be obtained from polymeric precursor nanofibers mainly from polyacrylonitrile (PAN) nanofibers through a heat treatment process of electrospun nanofibers. PAN-based fibers have been found to be the most suitable precursors for producing high-performance carbon fibers (compared to pitch, rayon, etc.) generally because of its higher melting point and greater carbon yield (>50 % of the original precursor mass) [23].

In contrast to CNTs/CNFs produced by CVD or other aforementioned methods, electrospun CNFs have integrated network structure and hence can be used as substrate/scaffold for neural tissue engineering with no need to be deposited on a substrate or be composited or grafted with a polymer. Furthermore, the diameter and surface morphology of electrospun CNFs can be easily controlled by controlling electrospinning of precursor polymer. On the other hand, toxic metal catalyst is not used in the synthesizing process of electrospun CNFs. Despite these advantages and favorable features of electrospun CNFs, there are a few studies on application of electrospun CNFs for neural tissue engineering applications. In first attempt in this field, Jain et al. investigated the cytocompatibility of electrospun CNFs using neuroblastoma and Schwann cells. Their results demonstrated good biocompatibility of the PAN-derived electrospun carbon nanofibers with nerve-tissue-specific cell types. A greater cell adhesion and proliferation of neuroblastomas cells on electrospun carbon nanofibers than on flat carbon films were also reported. They suggested that the electrospun carbon nanofibrous scaffolds can be used as a suitable biomaterial substrate in the context of their applications as artificial nerve implants [24]. In another study to address the cytotoxicity and cell fate processes of neural cells from the perspective of neural tissue engineering applications, Jain et al. investigated in vitro cytocompatibility of PAN-derived continuous carbon nanofibers. This study also suggested that electrospun carbon nanofibers are not cytotoxic in vitro and do not significantly induce apoptosis of Schwann cells but, in fact, even facilitate their proliferation and growth [25].

On the other hand, using proper cell along with substrate is critical for neural tissue regeneration. Among different cells used for neural tissue regeneration, human endometrial stem cells (hEnSCs) showed many advantages to be used as cell source in neural regenerative applications. hEnSCs are multipotent stem cells with the ability to differentiate into a number of cell lineages especially to neuron cells [26–29].

We investigated the proliferation and neuronal differentiation of hEnSCs on electrospun PAN-derived carbon nanofibers. PAN was first electrospun to form precursor polymeric nanofibers with random and aligned topographies. The nanofibers were then heat-treated to form carbon nanofibers. The differentiation of hEnSCs on random and aligned CNFs under neuronal induction medium was investigated by evaluating expression of neuron-specific markers at messenger RNA (mRNA) and protein levels by real-time PCR and immunocytochemistry, respectively. The morphology and proliferation of hEnSCs on electrospun CNFs were also investigated by SEM imaging and total lactate dehydrogenase (LDH) activity assay, respectively.

Experimental

Preparation of PAN Nanofibers

Polyacrylonitrile (PAN, average molecular weight (MW)=80,000 g/mol, Polyacryl, Iran) solution was prepared by

dissolving PAN in N,N-dimethylformamide/acetone (9:1 *v/v*) at 70 °C under magnetic stirrer to obtain 10.0 wt% solution as spinning solution. The electrospinning process was carried out using an electrospinning equipment (Electroris, FNM, Tehran, Iran). The spinning solution was kept in a standard 5-ml syringe that was connected to an 18-gauge stainless steel needle with inner diameter of 0.8 mm. The needle was connected to a positive high-voltage power supply. An aluminum foil was wrapped on the Electroris grounded rotating drum as collector and was located at the distance of 12.0 cm from the needle. The electrospinning was carried out by applying a high voltage of 13.0 kV between the needle and the rotating collector with diameter of 13 cm. The speed of drum was set at 400 and 2500 rpm to produce random and aligned nanofibers, respectively. The spinning processes were performed at 35 °C under room humidity.

Stabilization and Carbonization of PAN Nanofibers

The electrospun PAN nanofibrous mats with thickness of 90–100 μm were peeled from the aluminum foil and was heat-treated to produce carbon nanofibers. Stabilization and carbonization of PAN electrospun mats were done in a tube furnace (Azar, TF5/25–1720, Iran). Stabilization was performed in air at 290 °C with heating rate of 1 °C/min and holding at 290 °C for 3 h. The stabilized nanofibers were then carbonized at 1000 °C under high-purity nitrogen atmosphere (N_2 99.9999 %, Air Products). The samples were heated at the rate of 5 °C/min and kept for 30 min at 1000 °C [30].

Characterization of Nanofibers

Size and morphology of electrospun nanofibers were examined by scanning electron microscope (Philips, XL 30) after sputter coating with gold.

X-ray diffraction (XRD) was performed to investigate the crystalline structure of electrospun carbon nanofibers. XRD pattern of electrospun carbon mats was obtained from a PANalytical X'pert diffractometer using Cu Kα radiation (λ=0.1540598 nm) as the source.

Raman spectroscopy was performed using a SENTERRA (BRUKER, Germany) spectrometer using the 785-nm laser diodes and power of 25 mW under ambient conditions with a charge-coupled device (CCD) detector. The spectral resolution was <3 cm^{-1} and confocal depth resolution was 2 μm.

Human Endometrial Stem Cell Isolation and Culture

Human endometrial stem cells (hEnSCs) were isolated and purified from human endometrial tissue according to the previously described protocol [31]. Briefly, human endometrial tissue from healthy women was obtained in accordance with the Tehran University of Medical Sciences ethic committee. The tissue was digested in Hank's balanced salt solution (HBSS; Sigma, USA, H-6136) containing collagenase type I (1 mg/ml, Sigma-Aldrich) at 37 °C for 60 min. The resulting cell suspensions were neutralized with Dulbecco's modified Eagle's medium/F12 (DMEM/F12) medium (Gibco) containing 10 % fetal bovine serum (FBS; Gibco) and passed through a 70-μm sieve (BD Biosciences, USA, 93070). The cell suspensions were centrifuged, and the pellet of stromal cells was then suspended in a medium consisting of DMEM/F12 containing 10 % FBS and 1 % penicillin/streptomycin (50 U/ml penicillin and 50 U/ml streptomycin; P/S; Sigma-Aldrich). The media were changed every 3 days. Human EnSCs at the passage 3 after identification were used for the experiments.

Cytotoxicity and Proliferation of hEnSCs on CNFs

The cytotoxicity of CNFs and the proliferation of hEnSCs on electrospun CNF mats were determined using lactate dehydrogenase (LDH) assay kit (LDH Cytotoxicity Detection Kit^{PLUS}, Roche). The assays were done at three different incubation times as 24, 48, and 72 h for cytotoxicity assay and 1, 3, and 6 days for proliferation test. Electrospun CNFs were first punched circularly and put on the bottom of the 96-well plates so that the entire surface of the well was covered. After sterilization with 70 % ethanol for 2 h, the mats were washed with phosphate-buffered saline (PBS, pH=7.4) several times. For cytotoxicity assay, a number of 10,000 cells were seeded on the triplicates of carbon mats and tissue culture plate (TCP), as a control, in 100 μl of DMEM/F12 medium supplemented with 1 % FBS and 1 % antibiotic (50 U/ml penicillin and 50 U/ml streptomycin), and then the plate was incubated for various incubation time frames. It should be noted that culture medium was replaced with fresh medium after each 24 h for cytotoxicity tests of 48 and 72 h. For example for 48-h cytotoxicity test, the medium was replaced with fresh medium after first 24-h incubation, and for 72-h cytotoxicity test, the medium was replaced with fresh medium after 14 and 48 h.

For proliferation assay, a number of 5000 cells/well were seeded in 100 μl of DMEM/F12 medium supplemented with 10 % FBS and 1 % antibiotic, and then the plate was incubated at 37 °C in a CO_2 incubator (5 % CO2 and 90 % humidity) for various incubation time frames. For proliferation test, the supernatant medium was removed, and after washing with PBS, the cells were lysed with the lysis solution (5 μl/100 μl culture medium) after each incubation time, and the total LDH released activity was measured for all samples (experiment and control).

The cytotoxicity and proliferation were determined according to the procedure described by the manufacturer. The kit measures LDH activity released from the cytosol of damaged/lysed cells based on colorimetric assay. The amount of enzyme activity detected in the culture supernatant corresponded to the proportion of lysed cells.

Cytotoxicity and proliferation were determined according to the following Eqs. 1 and 2, respectively:

$$Cytotoxity\,(\%) = \frac{exp.\,value - low\,control}{hig\,control - low\,control} \times 100 \quad (1)$$

Low control determines the LDH activity released from the untreated cells. Here low control was the cells cultured on TCP.

High control determines the maximum releasable LDH activity in the cells. Here the high control was the cells cultured on TCP and were lysed by adding lysis reagent of the kit at the end of each culture period.

The results are given as relative values to the negative control in percent, whereas negative control (TCP) is set to be 0 % cytotoxic:

$$Proliferation\,(\%) = \frac{exp.\,value}{control\,value} \times 100 \quad (2)$$

Control for proliferation test was TCP.

The results of proliferation are given as relative values to the control (TCP) in percent, whereas the proliferation of cells on control is set to 100 %.

Differentiation of hEnSCs into Neuron-Like Cells on CNFs and TCP

To investigate the differentiation of hEnSCs on aligned and random electrospun CNFs, the carbon mats were first punched into the size of a well of a 48-well plate and then putted on the bottom of the wells. Mats were sterilized with ethanol 70 % (*v/v*) for 2 h and washed with PBS (pH=7.4) and DMEM/F12 medium several times to remove any residual ethanol. To induce neuronal differentiation, hEnSCs were seeded at 7000 cells/well on carbon mats and TCP. The cells were first incubated with DMEM/F12 medium supplemented with 10 % FBS, 100 U/ml penicillin, and 1 mg/ml streptomycin for 24 h. Differentiation of cells was induced by exposing them to a preinduction medium composed of DMEM/F12 (1:1), 20 % FBS, 2 % B27, 10 ng/ml fibroblast growth factor 2 (FGF2), 250 μM isobutylmethylxanthin, and 100 μM 2-metcaptoethanol and incubating them for 24 h at 37 °C and 5 % CO_2 to induce differentiation of cells to neuroepitheliom [26]. The treated cells were then cultured in induction media containing DMEM/F12 (1:1), 1 % B27, and 1 μM retinoic acid (RA) for 1 week. Then, the induced media were replaced with a medium composed of DMEM/F12 (1:1), 0.2 % B27, 100 ng/ml glial-cell-derived neurotrophic factor (GDNF), and 100 ng/ml brain-derived neurotrophic factor (BDNF), and 1 μM RA for another 1 week. As negative control, hEnSCs were cultured on TCP in the DMEM/F12 (1:1) supplemented with 10 % FBS for 15 days.

Immunocytochemistry

The hEnSCs grown on aligned and random carbon nanofibers and TCP under neuronal induction media for 15 days were investigated by immunocytochemistry of neural-specific markers including nestin, neurofilament 200-kDa subunit (NF-H), β-tubulin III (Tuj-1), glial fibrillary acidic protein (GFAP), and oligodendrocyte transcription factor (OLIG2). For immunofluorescence staining, the cells were fixed in 4 % paraformaldehyde for 1 h at room temperature, washed with PBS, and then permeabilized with 0.2 % Triton X-100 in PBS for 30 min at room temperature. The cells were blocked for 30 min at room temperature with 5 % bovine serum albumin (BSA) and incubated with primary antibodies against nestin (neural progenitor marker, mouse monoclonal antihuman, abcam 22035, 1/200), NF-H (neuronal marker, mouse monoclonal antihuman; abcam 7795, 1/200), beta-tubulin III (neuronal marker, mouse monoclonal antihuman; abcam7751, 1:500), GFAP (astrocyte marker, mouse monoclonal antihuman; abcam 4648, 1:200), and OLIG-2 (oligodendrocyte marker, goat polyclonal antihuman, Santa Cruz 19966, 1:200) diluted in 5 % BSA in PBS overnight. Secondary antibodies included Alexa Fluor 488 donkey anti-mouse (Invitrogen A-21202, 1:500) or Alexa Fluor 488 donkey anti-goat (Invitrogen A-11055, 1:500) or Alexa Fluor 594 donkey anti-mouse (Invitrogen A-21203, 1:700), and the nuclei were counterstained with 4',6-diamidino-2-phenylindole dihydrochloride (DAPI, Sigma-Aldrich,). A counterpart control treated with secondary antibody (lack of primary antibodies) was considered for each sample to be sure that the observed fluorescence of the differentiated cells is not autofluorescence. The immunofluorescence microscopy was performed using an OPTIKA fluorescence microscope.

Quantitative Real-Time PCR

The messenger RNA (mRNA) expression patterns of neuronal markers were analyzed by quantitative real-time PCR in treatment groups. Total RNA was extracted using EZ-10 Spin Column Total RNA Minipreps Super Kit (BIO BASIC INC). Complementary DNA (cDNA) synthesis from 1 μg of RNA was performed by PrimeScript™ first strand cDNA Synthesis Kit (TaKaRa). Quantitative real-time PCR reactions were carried out on StepOne™ Real-Time PCR machine (Applied Biosysytems) using primers listed in Table 1. cDNA was used for 40-cycle PCR using SYBR® Premix Ex Taq ™ II (Tli RNaseH Plus) (TaKaRa). Each reaction was repeated three times and relative fold change expression was quantified using the ddCt method. All Ct values calculated from the target genes were

Table 1 Primers used for real-time RT-PCR

Gene	Primer sequence (5′–3′)	Annealing (°C)
Nestin	F CAGAGGGAAGGAGATGAGTC R TGAGATGGAGCAGGCAAGAG	56
NF-H	F CGACATTGCCTCCTACCAG R CCGACACTCTTCACCTTCC	53
TUJ 1	F CAATTTCATCTTTGGTCAGAGTGG R TAGGTCTCATCCGTGTTCTCC	54
OLIG-2	F GGCAGTGGCTTCAAGTCATC R TCACCAGTCGCTTCATCTCC	54
GFAP	F CCCAGCAACTCCAACTAACAAG R TCTCCTTCCTCCTCATTCTAACG	55
GAPDH	F TCGCCAGCCGAGCCA R CCTTGACGGTGCCATGGAAT	55

normalized to GAPDH and calibrated using calculation from the undifferentiated human EnSCs as control group for analysis.

Statistical Analysis

All the data are presented as mean±standard deviation (SD). The data of cytotoxicity and proliferation assays were analyzed using one-sample *t* test, and differences from the control for each sample (random CNFs or Aligned CNFs) were considered statistically significant at p value <0.05. Analysis of variance (ANOVA) was used to compare the means in real-time PCR analysis, and a value of $p<0.05$ was considered statistically significant.

Results

Characterization of Electrospun Carbon Nanofibers

Electrospun carbon nanofibers were obtained after carbonization of PAN nanofibers as the precursor polymer. Size and morphology of the electrospun PAN and carbon nanofibers were studied using SEM images. Figure 1 represents the SEM images of random and aligned PAN nanofibers and their counterpart carbon nanofibers (Fig. 1a–d). The PAN nanofibers were shown to be straight and continuous without any beads in the structure (Fig 1a, b). The average diameter of PAN nanofibers was 174±31 and 165±20 nm for random and aligned fibers, respectively. As shown in Fig. 1d, the electrospun carbon nanofibers prepared in this study had reasonably good alignment for aligned nanofibers. In comparison with the SEM micrograph of PAN nanofibers, some structural deformations were observed for carbon nanofibers. In this case, some fusions between adjacent individual nanofibers (shown with arrows in Fig. 1c, d) were observed. Additionally, noticeable changes in the nanofiber diameter could be noticed after the carbonization step. The diameters were reduced to 154±25 and 145±27 nm for random and aligned carbon nanofibers, respectively.

The Raman spectrum and XRD pattern of electrospun CNFs are shown in Fig. 2. Raman spectroscopy is a valuable tool for studying the structural properties of carbonaceous materials. The characteristic D and G bands of CNFs appeared at 1313 and 1600 cm^{-1}, respectively (Fig 2a). The G band is

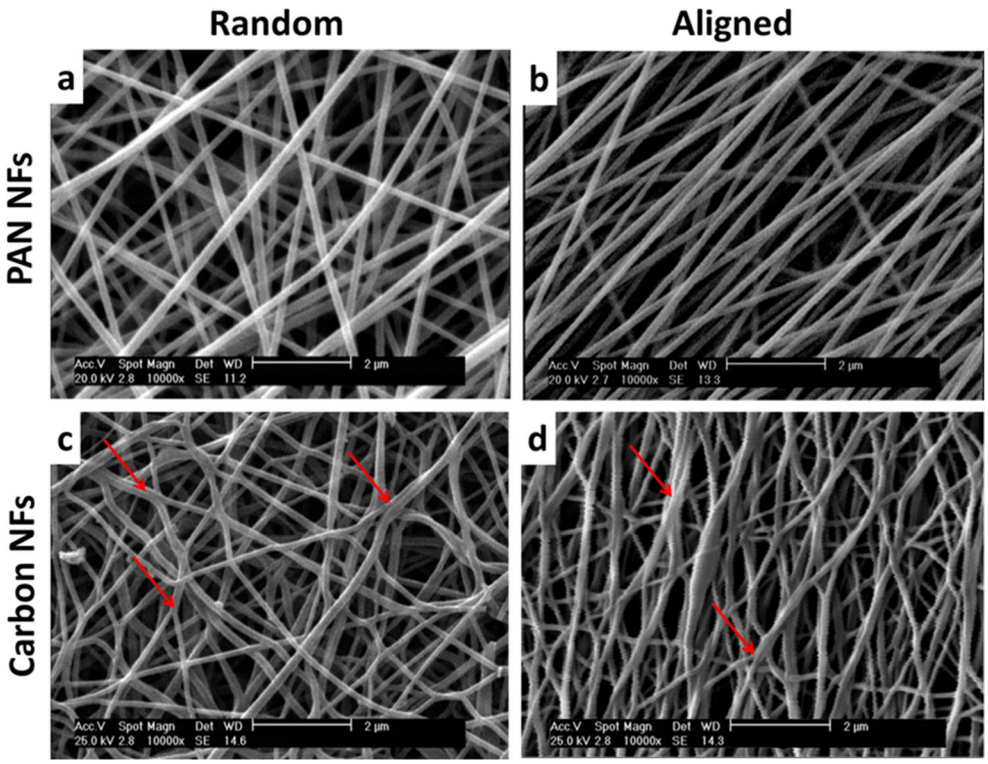

Fig. 1 SEM images of **a** random PAN nanofibers, **b** aligned PAN nanofibers, **c** random carbon nanofibers (CNFs), and **d** aligned carbon nanofibers. *Red arrows* show fusions between adjacent nanofibers in CNFs. Images were taken at ×10,000 magnifications (Color figure online)

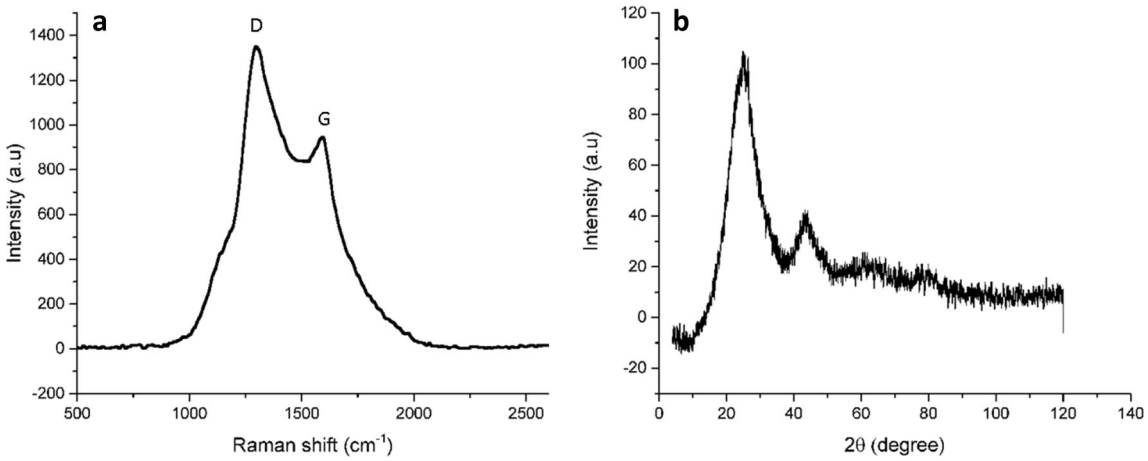

Fig. 2 Raman spectrum (**a**) and XRD pattern (**b**) of electrospun carbon nanofibers

related to the in-plane stretching vibration of the sp^2 carbon bonds within the ordered graphitic layers of fibers while the D band is related to the defects in the graphene structure or due to the edges present in the graphitic structure [32, 33]. The ratio of the integrated intensity of the D and G peaks ($R=I_D/I_G$) were calculated after Gaussian–Lorentzian mixed peak fitting of Raman spectrum. The R value of prepared carbon nanofibers was 0.95, which indicates some disorders in the carbon nanofibers. According to literature, more highly ordered carbon nanofibers have lower R values [34, 35].

XRD analysis was carried out to investigate crystalline structures in the prepared carbon nanofibers. The XRD pattern of electrospun CNFs is shown in Fig. 2b. The diffraction peak centered at the 2θ value of 25.15° is attributed to the crystallographic plane of (002) in graphite crystallites [35]. Additionally, a broad peak around 2θ value of 44°, corresponding to (100) layers, could be attributed to the graphite basal plane [36]. The average interplanar spacing, $d_{(002)}$, and crystallite size parameter, L_c, were determined from XRD spectra using the "Bragg equation" and the "Scherrer equation," as shown in Eqs. 3 and 4, respectively [35]:

$$d_{(002)} = \frac{\lambda}{2\sin\theta} \tag{3}$$

$$L_c = \frac{0.91\lambda}{\beta\cos\theta} \tag{4}$$

where "θ" is the scattering angle, "λ" is the wavelength of the X-ray used, and "β" is the width at half-maximum intensity (FWHM) of the (002) peak in radians. The prepared carbonized PAN nanofibers had the "L_c" and "$d_{(002)}$" values of 0.99 nm and 3.54 Å, respectively. The crystal size parameter was consistent with the reported values for 1000 °C carbonized electrospun PAN nanofibers [35]. The $d_{(002)}$ value of 3.54 Å in the prepared carbonized PAN nanofibers is larger than the $d_{(002)}$ value for graphite crystals (3.35 Å for highly oriented pyrolytic graphite (HOPG)) which is probably due to the presence of H, O, and N, and the presence of sp^3 bonds in the prepared CNFs [34]. The larger $d_{(002)}$ spacing indicates less ordered graphitic structures in the prepared carbon nanofibers than on HOPG.

Cytotoxicity and Proliferation of hEnSCs on Electrospun CNFs

In order to determine the cytotoxic effects of electrospun carbon nanofibers on hEnSCs, LDH assays were carried out by measuring the activity of released LDH from damaged cells with a spectrophotometer. The amount of LDH in cell supernatant is directly proportional to the number of cells with damaged membranes. As is shown in Fig. 3, aligned CNFs did not show any significant cytotoxicity difference, when compared to control (tissue culture plate, TCP), independent

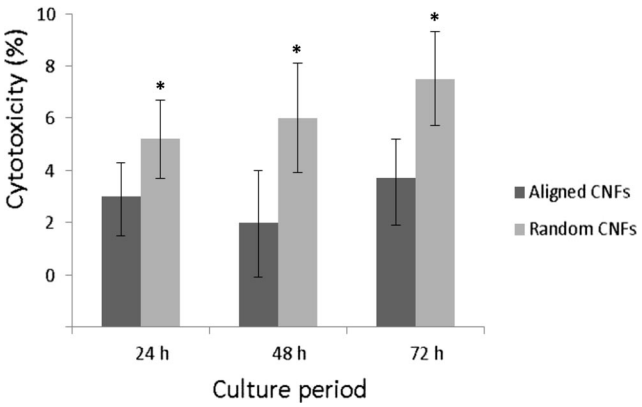

Fig. 3 Determination of cytotoxic effects of aligned and random electrospun carbon nanofibers (CNFs) on human endometrial stem (hEnSCs) measured by lactate dehydrogenase (LDH) assay. hEnSCs seeded on CNFs with a density of 10,000 cells/well in a 96-well plate and incubated for 24, 48, and 72 h. Data represented as mean±SD, $n=5$. The results are given as relative values to the negative control (tissue culture plate, TCP) in percent, whereas negative control is set to be 0 % cytotoxic. *Asterisk* indicates significant difference compared to control (TCP)

of the incubation period. However, random CNFs showed significant cytotoxic effect on hEnSCs in all cell culture periods ($p<0.05$). However, the cytotoxic effects of random CNFs were less than 10 % even after 72-h culture period. These results indicated proper cytocompatibility of electrospun carbon nanofibers with hEnSCs.

To investigate hEnSC proliferation on electrospun carbon nanofibers, the activity of total LDH was measured after complete cell lysis. Higher LDH activity is related to the higher number of cells on CNFs or on TCP. The results of cell proliferation on random and aligned CNFs are shown in Fig. 4. The results showed that both aligned and random CNFs reduced the proliferation of hEnSCs after 6 days of cell culture in comparison with the control (TCP). However, the effect of aligned CNFs were more considerable than that of the random CNFs. Random CNFs did not show any statistically significant difference in hEnSC proliferation after 1 and 3 days of culture period ($p<0.05$). However, the proliferation of hEnSCs on random CNFs after 6 days of cell culture was 93 % of the control ($p<0.05$). Aligned CNFs were more effective in reducing hEnSC proliferation. The proliferation of hEnSCs on aligned CNFs was 88 % and 76 % of the control after 3 and 6 days of culture period, respectively (with $p<0.05$ with respect to the control).

Immunocytochemistry of Differentiated hEnSCs on Electrospun CNFs

Human EnSCs were seeded on random and aligned CNFs and were treated with the neuron induction medium for 15 days. Immunocytochemistry of neural markers was carried out to investigate the differentiation of hEnSCs. Immunofluorescence staining was performed to characterize the expression of nestin (neural stem/progenitor cell marker), NF-H (neuronal marker), Tuj-1 (neuronal marker), Olig-2 (oligodendrocyte marker), and GFAP (astrocyte marker). The immunofluorescence images of differentiated hEnSCs on CNFs and on TCPs in comparison with negative control are shown in Fig. 5. The immunocytochemistry showed the expression of the immature neuronal marker (nestin) by some hEnSCs seeded on random CNFs and TCPs after 15-days treatment in neuronal induction media. As Fig. 5 clearly shows, the number of cells, which expressed nestin marker, was higher on random CNFs than those on aligned CNFs and TCPs. The differentiated cells were also found to express the neuronal proteins, NF-H and Tuj-1, on both CNFs and on TCPs after 15-day treatment in neuronal induction media. The NF-H- and Tuj-1-positive cells on aligned CNFs elongated along a preferred axis while NF-H- and Tuj-1-positive cells on random CNFs and TCPs oriented in several directions. Immunostaining of the hEnSCs seeded on random CNFs, aligned CNFs, and TCPs after 15-day treatment in neuronal induction media was negative for GFAP and Olig-2 (data not shown).

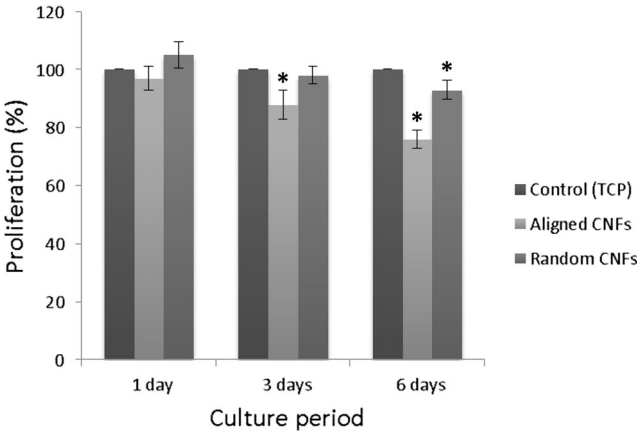

Fig. 4 Proliferation of human endometrial stem (hEnSCs) on aligned and random carbon nanofibers (CNFs) in proliferative medium measured by total lactate dehydrogenase (LDH) activity assay. hEnSCs seeded on CNFs with a density of 5000 cells/well in a 96-well plate and incubated for 1, 3, and 6 days. LDH activity was measured after cell lysis. Data represented as mean±SD, $n=5$. The results are given as relative values to the control (tissue culture plate, TCP) in percent, whereas the proliferation of cells on control is set to 100 %. *Asterisk* indicates significant difference compared to control (TCP)

Quantitative Real-Time PCR

Quantitative real-time PCR was performed in order to investigate neural marker expression in mRNA level, quantitatively. The results for hEnSCs seeded on CNFs and on TCPs and treated in neuronal induction media for 15 days are shown in Fig. 6. This figure indicates that the differentiation of hEnSCs cultured on CNFs was significantly different from that on the TCPs. The cells cultured on random CNFs showed significant higher expression of nestin compared to those cultured on aligned CNFs and TCPs. On random CNFs, there was a 3-fold increase in the expression of nestin in comparison with aligned CNFs and 1.5-fold increase in comparison with TCP ($p<0.05$). The lowest expression of nestin was observed for aligned CNFs. On the other hand, hEnSCs cultured on aligned CNFs yielded the highest expression of neuronal markers, NF-H and Tuj-1, when compared to the TCP and random CNFs. Cells, cultured on aligned CNFs, demonstrated 1.7-fold and 1.4-fold increase in NF-H expression when compared to random CNFs and TCP, respectively ($p<0.05$). Similarly, the expression of Tuj-1 in the aligned CNFs was 2.6 times higher than that in the random CNFs and 1.6 times higher than that in the TCPs. In contrast, the oligodendrocyte marker expression in random CNFs was significantly higher than those in the aligned CNFs and TCP. There was no difference in the expression of astrocyte marker (GFAP) in all groups. These results implied that the microenvironment of aligned CNFs encouraged the development of neurons. While, random CNFs kept the cells in neural progenitor state and slightly encouraged oligodendrocyte development.

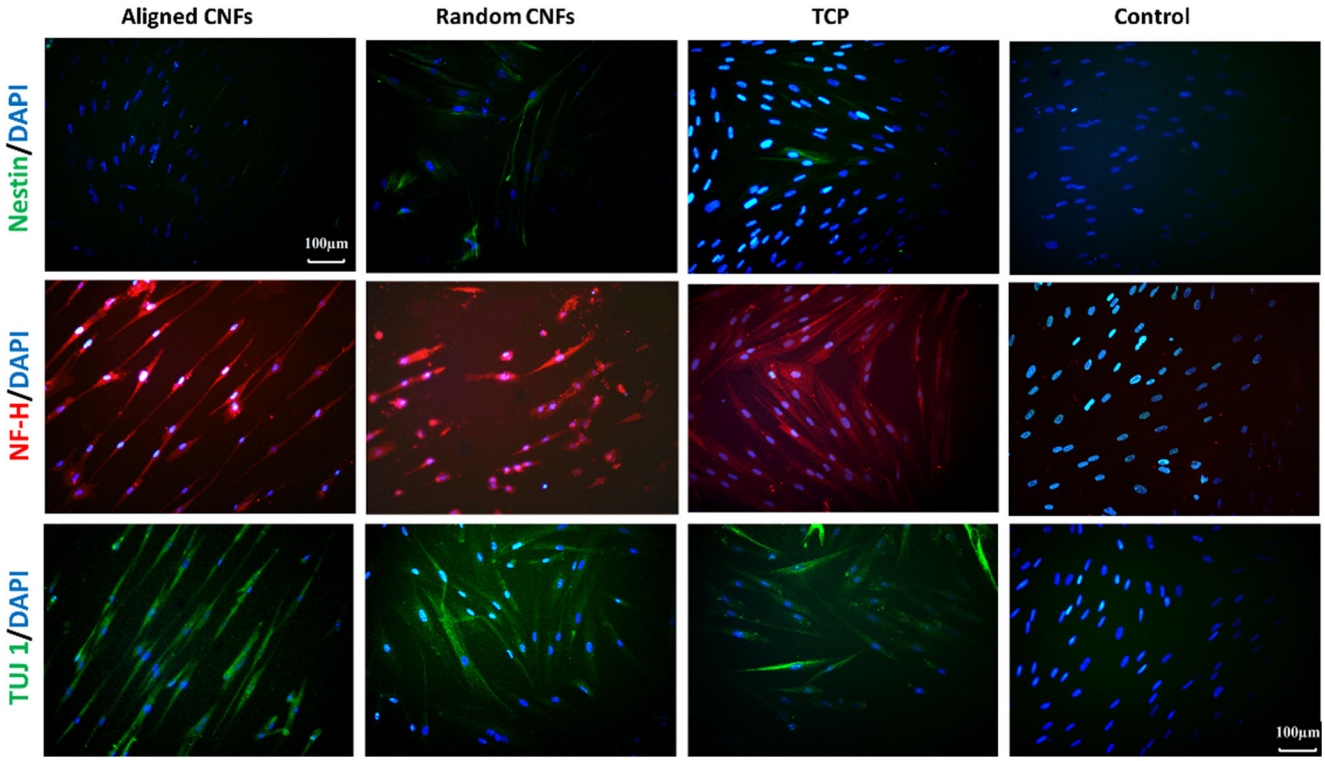

Fig. 5 Immunofluorescence staining of differentiated human endometrial stem cells (hEnSCs) on random CNFs, aligned CNFs, and tissue culture plate (TCP) after 15-day induction in neuronal medium. Cells were stained for neural markers including nestin, NF-H, and Tuj-1, and nuclei (*blue*) were stained using DAPI. Negative control was cells cultured on TCP in hEnSC normal media without neuronal induction factors (Color figure online)

SEM Morphology of Differentiated Cells on Carbon Substrates

The morphology of hEnSCs which were cultured on aligned and random CNFs after 15 days of treatment in neuronal induction media was investigated by SEM images. The SEM images of differentiated cells on aligned and random CNFs with different magnifications are shown in Fig. 7. According to this figure, cells were able to adhere to and spread on both random and align fibers. However, apparent changes in cell morphology were observed for cells cultured on aligned CNFs in comparison with cells on random CNFs. The cells cultured on aligned CNFs aligned along the main axis of the fibers (Fig 7a), while the cells cultured on random CNFs did not show any specific orientation (Fig 7d). Most cells cultured on aligned CNFs were long with a big round cell body and

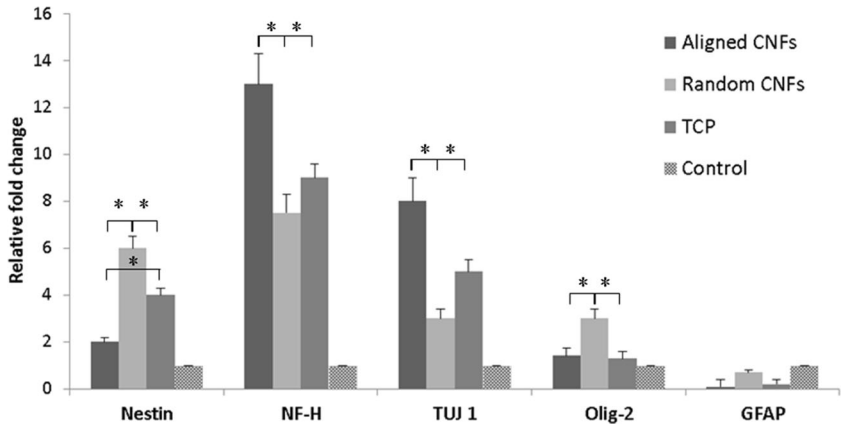

Fig. 6 Quantitative mRNA expression of neural markers in differentiated human endometrial stem (hEnSCs) on random CNFs, aligned CNFs, and TCP after 15-day induction in neuronal medium. The expression levels of each gene were normalized to GAPDH and calibrated using calculation from the undifferentiated human EnSCs as control group for analysis. Data represented as mean±SD, $n=3$. *Asterisk* indicates significant difference

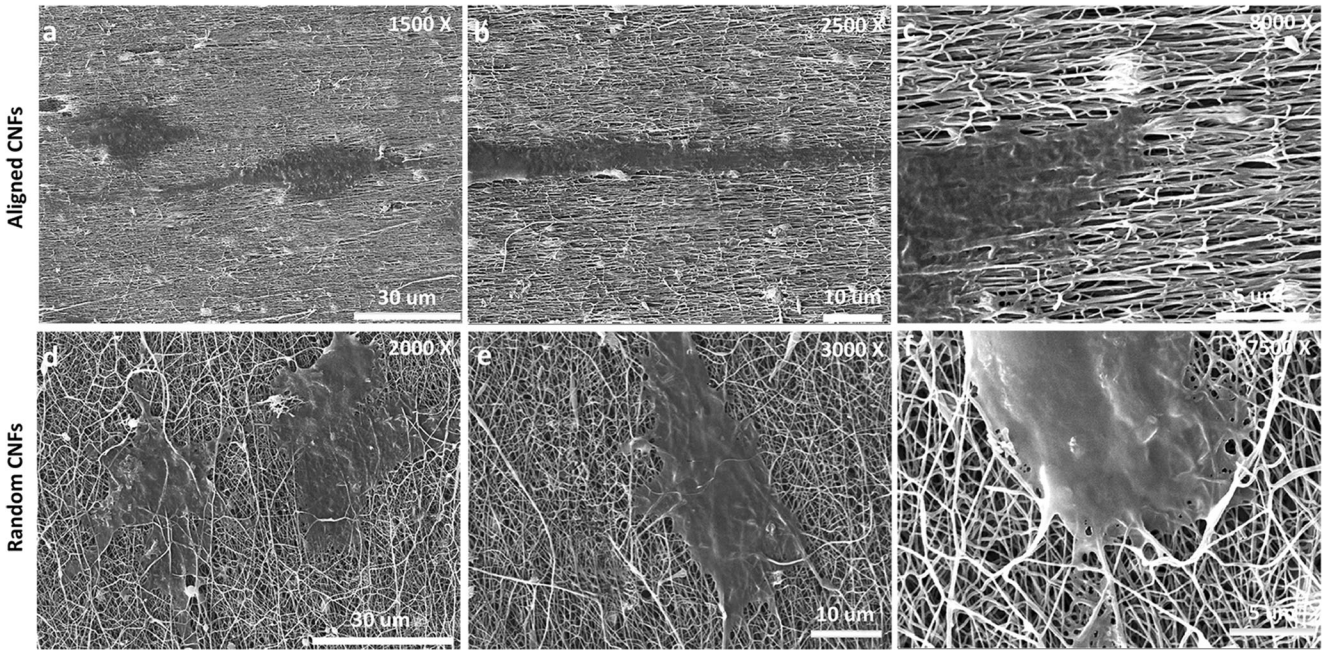

Fig. 7 Scanning electron microscopy images of human endometrial stem (hEnSCs) on carbon nanofibers (CNFs) after 15-day induction in neuronal medium at different magnifications; **a**, **b**, **c** cells on aligned CNFs with ×1500, ×2500, and ×8000 magnification, respectively. **d**, **e**, **f** cells on random CNFs with ×2000, ×3000, and ×7500 magnification, respectively

two long processes (Fig. 7a–c), while cells cultured on random CNFs were flatted round shaped and they extended in several directions (Fig. 7d–f). SEM images also illustrated the excellent adhesion and integration of differentiated EnSCs with both aligned and random CNFs (Fig. 7c, f).

Discussion

Electrospun CNFs can be considered as promising substrate for neural tissue regeneration, due to their electrical conductivity, structural integrity, simple patterning, and similarity to ECM. The biocompatibility of electrospun CNFs with neural-specific cells has been demonstrated in previous studies [24, 25]. In the present study, we investigated the proliferation and differentiation of hEnSCs on electrospun PAN-derived CNFs. PAN was used as polymeric precursor due to its suitability for producing high-performance carbon fibers (compared to pitch, rayon, etc.). PAN has higher melting point and greater carbon yield (>50 % of the original precursor mass).

Because of the easy availability of hEnSCs, their differentiation to functional neurons would be of interest to field of cell therapy [27]. Nevertheless, controlling cell proliferation and differentiation into specific neural cell lineage is still challenging. In addition to biochemical cues such as retinoic acid, physical cues such as surface topography are also important in differentiation of stem cells into specific neural cell lineages [37, 38, 26].

In the present study, the effects of electrospun CNF surface topography have also been investigated on hEnSC differentiation. Our results demonstrated that hEnSCs could attach, proliferate, and differentiate on electrospun CNFs. The surface topography of electrospun CNFs was also effective on hEnSC proliferation, morphology, and differentiation to neural cells. Aligned CNFs reduced the proliferation of hEnSCs compared to TCP and random CNFs. Aligned CNFs also induced a significant upregulation of neuronal markers, NF-H and Tuj-1, compared to random CNFs and TCP, hence suggesting the induction into neuronal lineage. In contrast, random CNFs maintained hEnSCs in neuronal progenitor state (indicated by higher expression of nestin) and upregulated the oligodendrocyte marker (oilg-2) in comparison with aligned CNFs and TCPs. The morphology of differentiated hEnSCs was also different on random and aligned CNFs. When the hEnSCs were cultured on aligned CNFs in neuronal induction media, the cells remarkably aligned and elongated along the direction of the CNFs main axis. However, the cells on random CNFs were not oriented in a particular direction. These findings established the importance of electrospun CNF nanotopographical cues on the neuronal differentiation of hEnSCs.

The significant effects of aligned nanotopography on enhancing stem cell differentiation into neuron-like cells have been previously demonstrated [38, 37]. Yim et al. demonstrated that aligned poly(dimethylsiloxan) (PDMS) nanogratings (350-nm width) significantly upregulated neuronal markers of human mesenchymal stem cells (hMSCs) compared to

unpatterned and micropatterned controls. They showed that the hMSCs also aligned and elongated along the nanograting axis [37]. The changes in hMSC neuronal marker expression were correlated with the elongation of cytoskeleton and nuclei. They suggested that aligned nanotopography induces neuronal differentiation of stem cells via changing stem cell morphology [37].

In another study, Lim et al. demonstrated that aligned polycaprolactone (PCL) nanofibers encourage neuronal differentiation of adult neural stem cells (ANSCs) upon induction of differentiation with retinoic acid compared to cells on random fiber or unpatterned surfaces. They also observed that ANSCs, which were cultured on aligned fibers, elongated along the major fiber axis [38]. It was demonstrated that aligned morphology was effective in upregulating canonical Wnt signaling pathway, which is crucial for neurogenesis in both embryonic and adult neural precursor cells [39]. Aligned nanofibers also had selectivity for neural cells. Aligned fibers were less receptive to the attachment and survival of oligodendrocytes compared to random fibers or unpatterned substrates. Substrate-induced elongation via upregulating canonical Wnt signaling and cell selectivity of aligned fibers was suggested as mechanisms to describe morphological control of stem cells fate [38].

Our results showed that aligned CNFs apparently changed the morphology of hEnSCs compared to random nanofibers. The hEnSCs cultured on aligned CNFs elongated along the fibers main axis (Figs. 5, 6, and 7). This biomechanical response may be transmitted to the nucleus through cytoskeletal-linked signaling pathways [38]. This may be a reason for enhancing neuronal differentiation of hEnSCS on aligned CNFs.

The proliferation of hEnSCs cultured on electrospun CNFs was also affected by CNF morphology. The proliferation of hEnSCs cultured on aligned CNFs was significantly less than that on random CNFs and on TCP after 3 and 6 days of cell culture in hEnSC proliferating medium (Fig. 4). The lower proliferation of hMSCs on nanopatterned PDMS compared to that on the unpatterned surfaces was also reported in Yim et al. study [37]. The upregulation of neuronal marker on aligned surface may be a result of reduced proliferation on aligned CNFs.

Moreover, conductivity of electrospun CNFs gives them additional advantage for regulating stem cell differentiation to neural cells in comparison with polymeric substrates. Electrical stimulation can be easily applied in the direction of CNFs axis to regulate stem cell behavior. It has been demonstrated that electrical stimulation can strongly influence stem cells to assume a neuronal fate [40]. This feature of electrospun CNFs along with their topographic effect on hEnSC elongation, proliferation, and differentiation suggest that this type of CNFs is a proper substrate for enhanced controlling of stem cell neuronal differentiation.

Conclusion

Differentiation of hEnSCs was investigated on electrospun carbon nanofibers with random and aligned topographies. Electrospun CNFs showed good biocompatibility with hEnSCs. The proliferation, morphology, and differentiation of hEnSCs were dependent on CNF topography. The aligned CNFs enhanced the differentiation of hEnSCs into neurons and also directed the cell growth along the fibers' axis. On the other hand, random CNFs kept the cells on neural progenitor state and slightly encouraged differentiation into oligodendrocyte. These findings suggest that electrospun CNFs are proper substrates for regulating stem cell differentiation into specific neural cell lineage for neural tissue regenerative applications.

Acknowledgments This project was supported by Tehran University of Medical Sciences (TUMS), grant No. 91-04-87-20021.

References

1. Nunes A, Al-Jamal K, Nakajima T, Hariz M, Kostarelos K (2012) Application of carbon nanotubes in neurology: clinical perspectives and toxicological risks. Arch Toxicol 86(7):1009–1020
2. Tran PA, Zhang L, Webster TJ (2009) Carbon nanofibers and carbon nanotubes in regenerative medicine. Adv Drug Deliv Rev 61(12):1097–1114
3. Wilkinson AE, McCormick AM, Leipzig ND (2011) Central nervous system tissue engineering: current considerations and strategies. Synthesis Lectures on Tissue Eng 3(2):1–120
4. Silva GA (2006) Neuroscience nanotechnology: progress, opportunities and challenges. Nat Rev Neurosci 7(1):65–74
5. Lee W, Parpura V (2009) Carbon nanotubes as substrates/scaffolds for neural cell growth. Prog Brain Res 180:110–125
6. Fraczek-Szczypta A (2014) Carbon nanomaterials for nerve tissue stimulation and regeneration. Mater Sci Eng C 34:35–49
7. Galvan-Garcia P, Keefer EW, Yang F, Zhang M, Fang S, Zakhidov AA, Baughman RH, Romero MI (2007) Robust cell migration and neuronal growth on pristine carbon nanotube sheets and yarns. J Biomater Sci Polym Ed 18(10):1245–1261
8. Hu H, Ni Y, Montana V, Haddon RC, Parpura V (2004) Chemically functionalized carbon nanotubes as substrates for neuronal growth. Nano Lett 4(3):507–511
9. Matsumoto K, Sato C, Naka Y, Kitazawa A, Whitby RL, Shimizu N (2007) Neurite outgrowths of neurons with neurotrophin-coated carbon nanotubes. J Biosci Bioeng 103(3):216–220
10. Ni Y, Hu H, Malarkey EB, Zhao B, Montana V, Haddon RC, Parpura V (2005) Chemically functionalized water soluble single-walled carbon nanotubes modulate neurite outgrowth. J Nanosci Nanotechnol 5(10):1707–1712
11. Tay CY, Gu H, Leong WS, Yu H, Li HQ, Heng BC, Tantang H, Loo SCJ et al (2010) Cellular behavior of human mesenchymal stem cells cultured on single-walled carbon nanotube film. Carbon 48(4): 1095–1104
12. Mattson MP, Haddon RC, Rao AM (2000) Molecular functionalization of carbon nanotubes and use as substrates for neuronal growth. J Mol Neurosci 14(3):175–182
13. Lovat V, Pantarotto D, Lagostena L, Cacciari B, Grandolfo M, Righi M, Spalluto G, Prato M et al (2005) Carbon nanotube

substrates boost neuronal electrical signaling. Nano Lett 5(6):1107–1110
14. Chao T-I, Xiang S, Chen C-S, Chin W-C, Nelson A, Wang C, Lu J (2009) Carbon nanotubes promote neuron differentiation from human embryonic stem cells. Biochem Biophys Res Commun 384(4):426–430
15. Kam NWS, Jan E, Kotov NA (2008) Electrical stimulation of neural stem cells mediated by humanized carbon nanotube composite made with extracellular matrix protein. Nano Lett 9(1):273–278
16. Dalby MJ, Gadegaard N, Tare R, Andar A, Riehle MO, Herzyk P, Wilkinson CD, Oreffo RO (2007) The control of human mesenchymal cell differentiation using nanoscale symmetry and disorder. Nat Mater 6(12):997–1003
17. Christopherson GT, Song H, Mao H-Q (2009) The influence of fiber diameter of electrospun substrates on neural stem cell differentiation and proliferation. Biomaterials 30(4):556–564
18. Malarkey EB, Fisher KA, Bekyarova E, Liu W, Haddon RC, Parpura V (2008) Conductive single-walled carbon nanotube substrates modulate neuronal growth. Nano Lett 9(1):264–268
19. Nguyen-Vu TB, Chen H, Cassell AM, Andrews RJ, Meyyappan M, Li J (2007) Vertically aligned carbon nanofiber architecture as a multifunctional 3-D neural electrical interface. Biomed Eng IEEE Trans on 54(6):1121–1128
20. McKenzie JL, Waid MC, Shi R, Webster TJ (2004) Decreased functions of astrocytes on carbon nanofiber materials. Biomaterials 25(7):1309–1317
21. Nataraj S, Yang K, Aminabhavi T (2012) Polyacrylonitrile-based nanofibers—a state-of-the-art review. Prog Polym Sci 37(3):487–513
22. Bhardwaj N, Kundu SC (2010) Electrospinning: a fascinating fiber fabrication technique. Biotechnol Adv 28(3):325–347
23. Rahaman M, Ismail AF, Mustafa A (2007) A review of heat treatment on polyacrylonitrile fiber. Polym Degrad Stab 92(8):1421–1432
24. Jain S, Sharma A, Basu B (2013) In vitro cytocompatibility assessment of amorphous carbon structures using neuroblastoma and Schwann cells. J Biomed Mater Res B Appl Biomater 101(4):520–531
25. Jain S, Webster TJ, Sharma A, Basu B (2013) Intracellular reactive oxidative stress, cell proliferation and apoptosis of Schwann cells on carbon nanofibrous substrates. Biomaterials 34(21):4891–4901
26. Ebrahimi-Barough S, Javidan AN, Saberi H, Joghataei MT, Rahbarghazi R, Mirzaei E, Faghihi F, Shirian S, Ai A, Ai J (2014) Evaluation of Motor Neuron-Like Cell Differentiation of hEnSCs on Biodegradable PLGA Nanofiber Scaffolds. Mol Neurobiol: 1–10
27. Mobarakeh ZT, Ai J, Yazdani F, Sorkhabadi SMR, Ghanbari Z, Javidan AN, Mortazavi-Tabatabaei SAR, Massumi M et al (2012) Human endometrial stem cells as a new source for programming to neural cells. Cell Biol Int Rep 19(1):7–14
28. Tavakol S, Aligholi H, Gorji A, Eshaghabadi A, Hoveizi E, Tavakol B, Rezayat SM, Ai J (2014) Thermogel nanofiber induces human endometrial-derived stromal cells to neural differentiation: in vitro and in vivo studies in rat. J Biomed Mater Res A 102(12):4590–4597
29. Tavakol S, Saber R, Hoveizi E, Aligholi H, Ai J, Rezayat SM (2015) Chimeric Self-assembling Nanofiber Containing Bone Marrow Homing Peptide's Motif Induces Motor Neuron Recovery in Animal Model of Chronic Spinal Cord Injury; an In Vitro and In Vivo Investigation. Mol Neurobiol: 1–11
30. Mirzaei E, Ai J, Sorouri M, Ghanbari H, Verdi J, Faridi-Majidi R (2015) Functionalization of PAN-based electrospun carbon nanofibers by acid oxidation: study of structural, electrical and mechanical properties. Fullerenes, Nanotubes, Carbon Nanostruct 23(11):930–937. doi:10.1080/1536383x.2015.1020057
31. Ebrahimi-Barough S, Kouchesfahani HM, Ai J, Massumi M (2013) Differentiation of human endometrial stromal cells into oligodendrocyte progenitor cells (OPCs). J Mol Neurosci 51(2):265–273
32. Zhang J, Loya P, Peng C, Khabashesku V, Lou J (2012) Quantitative in situ mechanical characterization of the effects of chemical functionalization on individual carbon nanofibers. Adv Funct Mater 22(19):4070–4077
33. Dongil A, Bachiller-Baeza B, Guerrero-Ruiz A, Rodríguez-Ramos I, Martínez-Alonso A, Tascón J (2011) Surface chemical modifications induced on high surface area graphite and carbon nanofibers using different oxidation and functionalization treatments. J Colloid Interface Sci 355(1):179–189
34. Zussman E, Chen X, Ding W, Calabri L, Dikin D, Quintana J, Ruoff R (2005) Mechanical and structural characterization of electrospun PAN-derived carbon nanofibers. Carbon 43(10):2175–2185
35. Zhou Z, Lai C, Zhang L, Qian Y, Hou H, Reneker DH, Fong H (2009) Development of carbon nanofibers from aligned electrospun polyacrylonitrile nanofiber bundles and characterization of their microstructural, electrical, and mechanical properties. Polymer 50(13):2999–3006
36. Wang G, Pan C, Wang L, Dong Q, Yu C, Zhao Z, Qiu J (2012) Activated carbon nanofiber webs made by electrospinning for capacitive deionization. Electrochim Acta 69:65–70
37. Yim EK, Pang SW, Leong KW (2007) Synthetic nanostructures inducing differentiation of human mesenchymal stem cells into neuronal lineage. Exp Cell Res 313(9):1820–1829
38. Lim SH, Liu XY, Song H, Yarema KJ, Mao H-Q (2010) The effect of nanofiber-guided cell alignment on the preferential differentiation of neural stem cells. Biomaterials 31(34):9031–9039
39. Gulacsi AA, Anderson SA (2008) β-catenin–mediated Wnt signaling regulates neurogenesis in the ventral telencephalon. Nat Neurosci 11(12):1383–1391
40. Yamada M, Tanemura K, Okada S, Iwanami A, Nakamura M, Mizuno H, Ozawa M, Ohyama-Goto R et al (2007) Electrical stimulation modulates fate determination of differentiating embryonic stem cells. Stem Cells 25(3):562–570